

Novel Anticoagulant from Date Palm Leaf/Cellulose Nano Whisker

Cintil Jose¹, Patrik Sobolciak², Igor Krupa², Mariam Al Ali AlMaadeed²

¹Department Of Chemistry, Newman College, Thodupuzha, Kerala, India

²Center Of Advanced Materials, Qatar University. P.O. Box: Doha, Qatar.

ABSTRACT: Nature inspires us to develop new high performance materials from its renewable resources and among these cellulose nanocrystals(CNCs) are most popular due to their unusual properties and resulting applications. In this work, cellulose nanocrystals were extracted by acid hydrolysis and the anticoagulant activity of surfaces decorated with cellulose nanocrystals is explored. Such surfaces bear a high amount of negatively charged sulfate groups, which mimic the naturally occurring anticoagulant heparin in terms of charge density. It is observed that CNC decorated surfaces significantly enhance the coagulation times of blood plasma and whole blood as studied from Quartz crystal microbalance with dissipation studies (QCM-D) and simple clotting tests. Cellulose nanocrystals bear a high amount of negatively charged sulphate groups which resemble the charge density of natural anticoagulant Heparin. Anticoagulant effect of functionalized cellulose nanocrystals was demonstrated by clinical test. This new material is potentially applicable in medicine as anticoagulant similarly as common heparin.

I. INTRODUCTION

Nature inspires us to develop new high performance materials from its renewable resources and among these cellulose nanowhiskers (CNCs) are most popular due to their unusual properties and resulting applications. The quest for new materials based on CNCs started in 1992 when the liquid crystalline nature of interacting colloidal cellulose suspensions was observed for the first time [1]. Cellulose nanowhiskers (CNCs) have emerged as a new class of nanomaterial for polymer reinforcement and nanocomposite formulation owing to their exceptionally high mechanical strength, low density, chemical tunability, environmental sustainability, and anticipated low cost. [2] Cellulose whiskers (nanowhiskers), obtained by acid hydrolysis of cellulose, are a more recent area of application for nanocomposites. In the acid hydrolysis process, the amorphous regions of cellulose are dissolved, yielding crystalline rod or whisker shape nanoparticles with diameters that range from 8 to 20 nm and lengths of 100 nm to few micrometers, depending on the source of the cellulose. These whiskers have a high modulus, high aspect ratio, and their surface chemistry can be modified to broaden their use in high-value applications [3-5]. Since cellulose and also cellulose nanowhiskers are [6] highly biocompatible and biodegradable, the potential of cellulose nanowhiskers to be used in medical materials has attracted very recently significant interest. A very important feature of CNCs in this respect is the wide range of surface functionalities that can be easily introduced into the material. The most widely used functional groups are sulfates, which are created in the course of the preparation of CNC, where sulfuric acid is added to microcrystalline cellulose at low temperatures [3].

The amorphous regions around the cellulose microfibrils could be destroyed by acid hydrolysis under controlled conditions, keeping the crystallites intact. The acid hydrolysis is selective in cellulose fibrils, resulting in colloid suspensions of cellulose nanowhiskers. Whiskers of cellulose are primarily obtained by acid hydrolysis, with strong acids such as sulphuric and hydrochloric, which leads to nanowhiskers ranging between 100 and 400 nm in length and less than 10 nm in width [7-9]. This treatment does not only remove amorphous domains of cellulose but also esterifies the surface of the remaining crystallites. When comparing the obtained sulfated CNCs with other naturally occurring polysaccharides, the similarity to heparin is reported [10]. This is because of the very high negative charge density of heparin due to the presence of sulfate groups. Anticoagulants have been used widely for blood treatment during dialysis and surgery and also for treatment of disseminated intravascular coagulation and thrombosis. Anticoagulants have also been proved useful as antithrombogenic ionic or covalent coatings for synthetic materials that come into direct contact with blood [11]. Considering the adverse effects of the existing anticoagulant therapy, there is a need to find out alternative drugs from natural origin as safe anticoagulant. Because of the anticoagulant efficiency, glycosaminoglycan heparin is effective for the treatment of thromboembolism disorders, but as it is originated from animal materials, it has the risk of contamination, osteoporosis, and inconsistent patient responses. Because of very expensive nature, synthetic heparin like ultra-low-molecular-weight heparins,[12] are also not a good alternative [12-15]. Therefore, there is a need to develop new synthetic materials that have a similar structure as heparin and can mimic the anticoagulant and antithrombogenic activity of heparin.

Date palm tree has played an important role in human activity in Arabic countries since before recorded history. It is extensively cultivated for its edible fruit and the palm tree forests of Arabic countries are highly regarded for their recreational, aesthetic, spiritual, and natural values. They are valued for providing wildlife, clean air and ameliorating global warming. *Phoenix dactylifera* L., date palm, is among the most important species in the Palm family (Arecaceae), which encompasses about 200 genera and more than 2,500 species [16-17]. Date palm leaves is a raw biomass material with high potential for manufacturing value added products. The utilization of biomass for processing of new materials has attracted growing interest because of their ecological and renewable nature characteristics. The main components of date palm leaves are cellulose, hemicellulose, lignin, solubles and moisture. The annual world production of dates has reached 6-8 million mt, representing a market exchange value of over 1 billion USD. In this work, date palm leaves were used as a source of cellulose whiskers which can be used as an anticoagulant. These cellulose nanowhisker are obtained from native cellulose sources by acid hydrolysis of native cellulose, which removes the amorphous regions. The remaining particle is individualized nanosize monocrystalline particles. This paper is structured as follows. (1) extraction of cellulose nanowhisker from date palm leaves by Sulphuric acid hydrolysis (2) detailed characterization of surface morphology (3) determination of sulphate charges by zeta potential measurements and (4) determination of red blood cell mobility.

II. EXPERIMENTAL

2.1 Materials

Date palm leaves were collected from local farms in Qatar was used for extracting the fiber. The various chemicals used for extraction of fiber and the preparation of nanowhisker are sodium hydroxide (NaOH), acetic acid (CH₃COOH), sodium chlorite (NaClO₂), and sulphuric acid (H₂SO₄). All reagents used were of analytical grade.

2.2 Cellulose nanowhisker production from date palm leaves

Dried palm leaves were grinded into short fibers and treated with 5wt % NaOH at a temperature of 110 °C for one hour. Then the fibers were washed in water, the fibers were bleached using a mixture of NaOH and acetic acid (27 and 78.8 g, respectively) and sodium chlorite solution. Bleaching was repeated three times. After bleaching, the fibers were thoroughly washed and dried. Fibers were then subjected to acid hydrolysis using sulphuric acid. Then, 270.3 g of water were added to 5.9 g of bleached fiber and mixed until good dispersion. Thereafter 529.7 g of sulphuric acid was slowly added to the suspension (65 wt. % acid concentration). The cellulose in the acid suspension was then hydrolyzed at 44 °C for 130 min under mechanical stirring. The excess of sulphuric acid was removed by repeated cycles of water exchange/centrifugations (5000 rpm) at room temp for 10 min, until the supernatant became turbid. After the centrifugation cycles, the suspension containing the CNC was washed in distilled water. Then the CNC suspension was homogenized using an Ultra-Turax T25 homogenizer and was subjected to ultrasound treatment in order to ensure dispersion of CNC. Finally, the neutralization was carried out by adding drops of a 1 wt. % NaOH solution to the CNC suspension. Suspensions were stored at 4 °C.

III. CHARACTERIZATION OF CELLULOSE WHISKERS.

3.1 Chemical composition

The chemical composition of the palm fibers at each stage of treatment was determined according to the ASTM standards [α-cellulose (ASTM D 1103-55T), hemicellulose (ASTM D 1104-56), lignin (ASTM D 1106-56), moisture content (ASTM D 4442-92)]. Yield of palm nanowhiskers was noted by the following equation.

$$\text{Yield \%} = \frac{W_1}{W_0} \times 100$$

Where W₀ is the weight of initial palm fibers taken first and W₁ is the weight of palm nanowhiskers obtained (dried).

3.2 Fourier transform infra-red spectroscopy (FTIR)

Fourier transform infrared spectra were recorded using a Shimadzu IR-470 IR spectrophotometer. Untreated, alkali-treated, bleached and acid-treated palm fiber samples were analysed. Prior to the experiment, fibers were dried in an air oven at 60°C for 12 hours. The FT-IR spectrum of each sample was obtained in the range of 400–4000 cm⁻¹. The KBr disk (ultrathin pellets) method was used and the experiments were carried out with a resolution of 2 cm⁻¹ and a total of 15 scans for each sample.

3.3 Scanning electron microscopy (SEM)

Scanning electron microscopy (JEOL JSM-820 model) was used to observe the surface morphology of the palm fibers. The effect of the different chemical treatments was assessed using a comparison of the untreated, alkali treated, bleached and acid treated fibers. The fibers were dried in an air oven at 60°C for 12 hours. The samples were then coated with gold using a vacuum sputter coater (model SC 500) to avoid subsequent charging before measurement by SEM.

3.4 Transmission electron microscopy (TEM)

Transmission electron microscopy (model Philips CM 200) was used to determine the dimensions of the cellulose nanowhiskers obtained from the palm fibers. A drop of a diluted suspension (1 wt%) was deposited on the surface of a clean copper grid and coated with a thin carbon film. As for contrast in TEM, the cellulose nanowhiskers were negatively stained in a 2 wt% solution of uranyl acetate. The sample was dried at ambient temperature before TEM analysis and the measurement was carried out with an accelerating voltage of 80 kV.

3.5 X-Ray diffraction technique (XRD)

X-ray diffraction was used to determine the crystallinity of the palm fibers after different treatments. Each material in the form of milled powder was placed on the sample holder and leveled to obtain total and uniform X-ray exposure. The X-ray equatorial diffraction patterns of the raw, alkali treated, bleached and acid treated fibrils were obtained with an X-ray diffractometer (JEOL diffractometer, Model JDX 8P) using CuK α radiation ($\lambda = 0.1539$ nm) at the operating voltage and current of 40 kV and 20 mA respectively. The X-ray diffractograms were obtained at room temperature within a 2 $^\circ$ range from 5 to 80 $^\circ$ and a scan rate of 2 $^\circ$ min $^{-1}$.

3.6 Zeta potential measurements

Potential charges which may be on the surface of nanowhisker in pure water were measured with a Malvern 3000 Zetasizer. A nanowhiskerline cellulose suspension (0.05 wt.%), previously sonicated for 5 min, was prepared and analyzed to determine the Zeta-Potential of nanofiber suspensions. Zeta potential measured as function of concentration of original aqueous palm cellulose suspension in 0.1 mM KCl electrolyte.

3.7 Determination of Red Blood Cell Mobility

This method, which was introduced and described by Lahootiet *al.* [18], is based on observation of red blood cell mobility when exposed to biomaterials surfaces using an optical microscope and image analyzer. Glass slides were rinsed with water and acetone and dried at room temperature. Next, the washed and dried slides were coated with cellulose nanowhiskers and the slides were again dried at room temperature. Two slides with the same coating were always used. A Feather $^\circ$ blood lancet was used to draw fresh whole blood, which was taken with a transfer pipette with a disposable tip to maintain sterile conditions. A few microliters of blood were put on one slide. With a second slide, the blood was distributed on the surface and this slide was put on the first one so that the blood was enclosed in-between the coated surfaces. Using an Olympus BX 51 microscope at 50 \times magnification, the erythrocytes were monitored in transmitted light and photos were taken with the program cell $^\circ$ D at each second. The program saves the time at the base of the image when a photo is taken. The clotting time determination method gives us important information about the coagulation of whole blood.

IV. RESULT AND DISCUSSIONS

4.1 Chemical composition

Table 1: Chemical composition of fibers at each stage of treatment (deviation up to 5%)

Fiber	Cellulose	Hemicellulose	Lignin	Moisture
Raw	34	26	30	7
Alkali treated	67	2	22	8
Bleached	86	0.5	1	9.5

The chemical composition of palm leaf fibers determined at each stage of treatment is summarized in Table 1. The sum of the percentage of cellulose, hemicellulose and lignin corresponds to the total dry matter, showing that there are other components like pectin, wax, moisture content, etc. The alkali treatment removes a certain amount of lignin, hemicellulose, wax and oils covering the external surface of the fiber cell wall. The alkali treated fiber is then subjected to bleaching. Bleaching of the alkali treated fiber was done to complete elimination of the remaining cementing materials from the fiber. Hemicellulose is a water soluble polysaccharide and lignin is a complex organic compound with alkali soluble character [19], Hence the percentage of lignin decreases from raw fiber to bleached fiber. After cellulose was prepared, acid hydrolysis was carried out in order to produce cellulose nano whiskers. The fine structure of cellulose materials is composed of crystalline and amorphous regions. The amorphous regions easily absorb chemicals such as dyes

and resins, whereas the compactness of the crystalline regions makes it difficult for chemical penetration [20]. The modification of plant fibers may involve the removal of the surface impurities, the swelling of the crystalline region, and removal of the hydrophilic hydroxyl groups. The common trend from the observation is the gradual decrease of amorphous components like lignin and hemicellulose from raw fiber to bleached fiber. The lignin will react with NaClO_4 and dissolve out as lignin chloride. It is clear from Table 1 that the raw fiber has the highest percentage of hemicellulose and lignin and the lowest percentage of cellulose. But when the fiber is subjected to alkali treatment followed by bleaching we can observe that there is a decrease in percentage of the hemicellulose and lignin and increase in percentage of cellulose. When the raw fiber is subjected to alkali treatment followed by bleaching, the hemicellulose is partly hydrolyzed and the lignin is depolymerized, giving rise to sugars and phenolic resin compounds that are partially soluble in water [21]. Generally, the pre-treatments ends up in a chemical reaction of glycosidic bonds within the hemicellulose and it results in the cleavage of hemicelluloses–lignin bonds [22]. The high solubility of lignin and hemicelluloses was because of the cleavage of the ether linkages between lignin and hemicelluloses by alkali treatment [23]. It was reported that a diluted alkali treatment was performed to solubilize lignin, pectin, hemicelluloses and proteins while bleaching was applied to remove the lignin residues [24–25]. The yield of INF with respect to the initial amount of dried palm fibers was 12%.

4.2 Fourier transform-infra red spectroscopy (FTIR) analysis

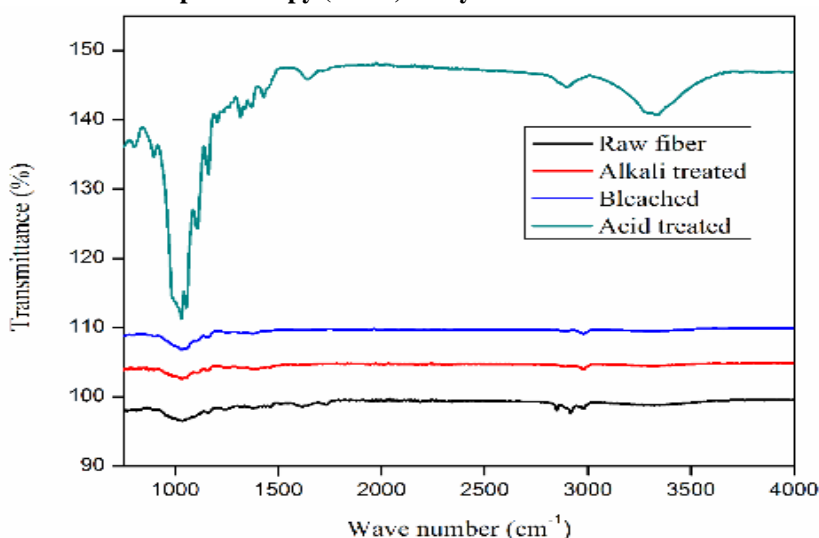


Figure 1: FTIR spectra of palm fibers at different stages of preparation.

FTIR spectroscopic analysis of the untreated (raw), alkali treated, bleached and acid treated palm fiber samples is given in Figure 1. Plant fiber consists of three main materials, cellulose, hemicellulose and lignin. These materials are mainly composed of alkanes, esters, aromatics, ketones and alcohols with different oxygen containing functional groups. Erdtman, Klemm and Oh have reported on the infrared spectra of cellulose, hemicellulose and lignin [26–29]. During isolation process, sulphate group is introduced in to the material. The cellulose nanowhiskers showed two characteristic absorption bands, one band at 879 cm^{-1} and one at 1264 cm^{-1} were observed, which was assigned to the symmetrical vibration of C–O–S and the asymmetric stretching vibration of $\text{O}=\text{S}=\text{O}$ [30]. However, these two absorption peaks were absent in the raw, alkali and bleached fibers, which proved that the sulfate group had been successfully introduced into the cellulose. The peak at 3300 cm^{-1} , which was observed in the spectra of all fibers, corresponds to the OH stretching vibrations of hydrogen bonded hydroxyl group and it shows the hydrophilic tendency of the fiber. Lignin presented characteristic peaks in the range $1200\text{--}1300\text{ cm}^{-1}$ corresponding to the aromatic skeletal vibration. In addition, due to the presence of functional groups such as methoxyl $-\text{O}-\text{CH}_3$, C–O–C and aromatic C=C, peaks in the region between 1830 cm^{-1} and 1730 cm^{-1} was observed. The peak at 893 cm^{-1} is due to the glycosidic linkages of glucose ring of cellulose, which appeared in all the spectra. This peak is more intense in bleached and acid treated fibers indicating that cellulose content increased by different treatments. The values obtained from the spectrum are in good agreement with the reports in the literature [31].

4.3 Scanning electron microscopy (SEM) analysis

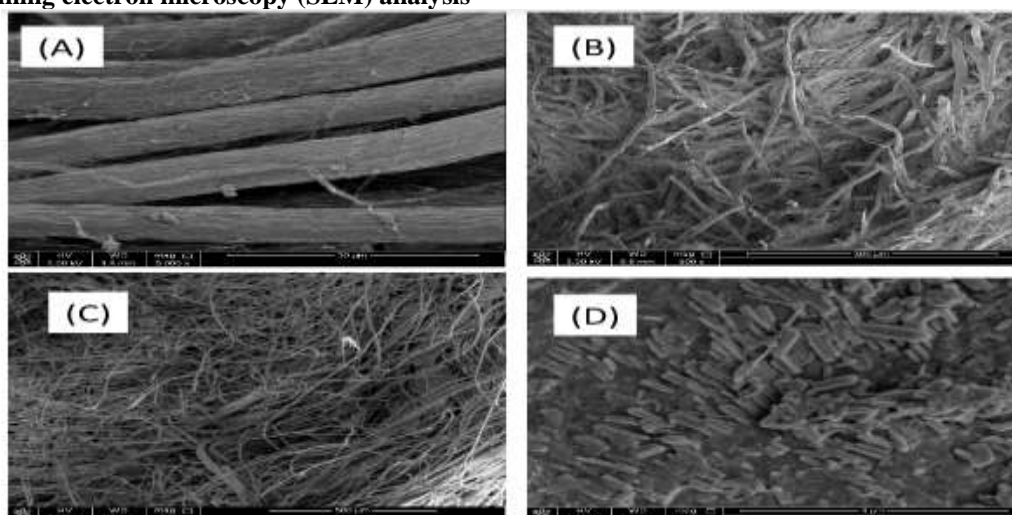


Figure 2: SEM image of (A) raw fiber (B) alkali treated fiber (C) bleached fiber and (D) acid treated fiber

Scanning electron microscopic analyses of treated and untreated palm leaf fibers in various forms were carried out to assess their surface morphology. Figure 2 (A) shows the raw palm leaf fiber, that s formed of cellulose-fiber conglomerates that were tightly joined by an intercellular matrix composed of hemicelluloses, lignin, and pectins. To extract cellulose fibers, hemicellulose, lignin, and pectins must be removed. Each fiber is composed by several microfibrils with diameters in micrometer range. Each elementary fiber shows a compact structure; exhibiting an alignment in the fiber axis direction with some non-fibrous components in the fiber surface [32-33]. Chemical pretreatments conduct to the partial removal of different components generating a diameter reduction by separating the macro into micro fibrils as well as a change in the fibers composition (cellulose purification). From the figure, it can be seen that in raw fiber, the fibrils are associated in bundles and the surface of the fiber is found to be smooth due to the presence of waxes and oil. The micrograph of alkali treated fiber Figure 2 (B) shows defibrillation. During alkali treatment, the hemicellulose is hydrolyzed and become water soluble and the lignin gets depolymerized. As a result, defibrillation of the fiber occurs because of the removal of the cementing materials which can be seen from the SEM images. The morphology of the bleached palm fiber is shown in figure 1(C). The cementing materials such as lignin and hemicellulose present in the fibers get dissolved out during alkali treatment and bleaching process. From Fig. the dissolution of the cementing materials from the fibers is shown more clearly; the fibers are separated into individual fibrils during the bleaching process. Upon bleaching the fibers get converted to numerous cellulose microfibrils. Bleaching helps to remove most of the lignin present in the leaf fiber, this helps in further defibrillation. Sodium hypochlorite and sodium acetate buffer allows the removal of lignin and tannin. Lignin is rapidly oxidized by chlorine. Lignin oxidation leads to lignin degradation and leads to the formation of hydroxyl, carbonyl and carboxylic groups, which facilitate the lignin solubilization in an alkaline medium. Partial removal of cementing components and defibrillations are important steps towards more efficient bleaching and subsequent steps of nanowhiskers hydrolysis. Acid treatment after bleaching process helps to disintegrate the fibrils further.

4.4 Transmission electron microscopy (TEM) analysis

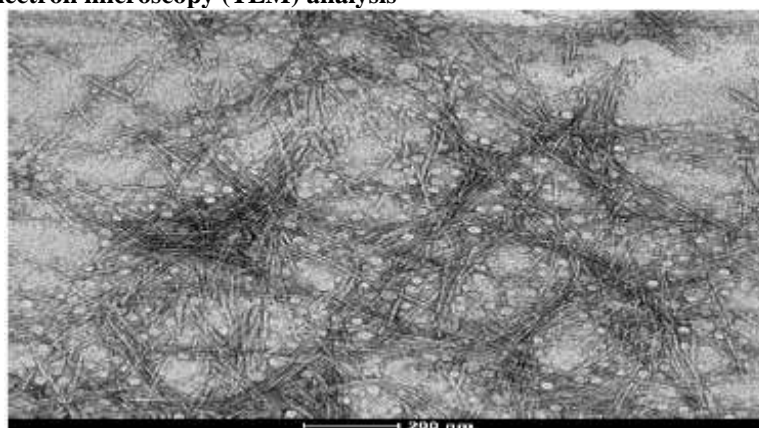


Figure 3: TEM micrograph of cellulose whiskers

The palm leaf fiber was subjected to chemical treatment to remove the non cellulosic constituents. This chemically treated mass, when subjected to acid hydrolysis, revealed a unique transformation and very fine cellulosic nanowhiskers were gradually released from fiber. Acid hydrolysis finally resulted in a white colloidal suspension and a solid residue that settled at the bottom. The colloidal suspension of cellulose particles was separated, made acid free and subjected to high speed homogenization. These whiskers were observed by TEM to obtain an accurate idea of shape and size of the cellulose whiskers. TEM analysis of the suspension revealed that, nanowhiskers have a needle like structure, and uranyl acetate staining give good contrast between the cellulose whiskers and the carbon film. Nanofibers are much more clearly defined probably because of the removal of pectic polysaccharides. These nanowhisker are individualized and some agglomerates are also observed. Because of the increased surface area and the expected high density of hydroxyl groups at the fibril surface, fiber bundles strongly interact and tend to agglomerate. The average diameter and length of cellulose nanowhiskers are in the range of 10-15 nm and 150-200 nm, giving good aspect ratio. High aspect ratio of cellulose whiskers results in a good reinforcing effect, resulting in good mechanical properties. And the aspect ratio may vary depending on the source and the preparation conditions. These images proved the efficiency of sulphuric acid hydrolysis, confirming that the aqueous suspensions contained cellulose nanowhiskers consisting mostly of individual fibrils of uniform length and some aggregates. This is consistent with the structural model proposed by Battista (1962) [34], and the results reported by Lai-Kee-Him et al. (2002) [35]. As reported by Dong et al. [36], the conditions of preparation govern somewhat the properties of the cellulose particles. The shortening of nanowhisker length is due to the prolonged acid attack, which remove amorphous molecules and partly destroy the crystalline portions of fibrils. Nanowhiskers isolated from palm leaves are a natural candidate for numerous medical applications because of its characteristics such as chemical structure, non toxicity, and biocompatible nature. The suspensions obtained after H_2SO_4 hydrolysis were very stable. The reason is that, the incorporation of sulfate groups on the cellulose surface created negative electrostatic layer resulting in a more stable final suspension. These negative charges make these whiskers more attractive for the application as anticoagulant.

4.5 X-ray diffraction (XRD) analysis

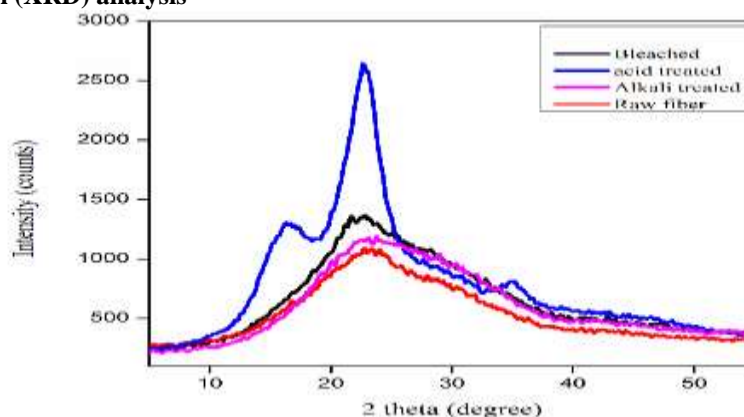


Figure 4: X-ray diffraction patterns of the raw, alkali treated, bleached and acid treated palm fiber

Cellulose crystallinity in individualized nanofibers is the key factor determining their mechanical and thermal properties. The hydrogen bonds between cellulose molecules are arranged in a regular system resulting in an ordered system with crystal-like properties. Individual fibrillar units consist of long periods of ordered regions (crystallites) interrupted by completely disordered regions. In native cellulose the length of the crystallites can be 100–250 nm with cross-sections of 3-10 nm. Any chemical or mechanical treatments affect the crystallinity of the cellulosic fibers. Therefore, we studied the crystallinity of the cellulose fibers before and after the chemical treatment. X-ray diffraction patterns of cellulose nanowhiskers compared with treated and untreated fibers, are presented in Figure. 4. From the XRD graphs, it is clear that the treated palm fibers show a crystalline nature. The fibers show increasing orientation along a particular axis as the fibers are treated under different processing conditions. The peak at $2\theta = 22^\circ$ is sharper for the chemically treated fibers than the untreated. The sharper diffraction peak is an indication of higher crystallinity degree in the structure of the treated fibers. The increase in the crystallinity of the chemically treated fibers is due to partial removal of the hemicelluloses and lignin during the chemical treatment. The increase in the number of crystallinity regions increases the rigidity of cellulose. The increase in crystallinity was undoubtedly due to the removal of hemicellulose and lignin, which exist in amorphous regions. This leads to the realignment of cellulose molecules removing amorphous components enables $-OH$ groups on cellulose surface to form new hydrogen bonds, increasing the crystallinity. From the pattern, it is clear that the raw fiber is almost amorphous with very

little crystallinity in it. As expected, untreated fibers showed a large amorphous portion due to their high lignin content (37% lignin), as previously mentioned. In raw fibre, crystalline cellulose components are embedded in the matrix of lignin, hemicellulose, pectin etc. During alkali treatment, the matrix materials react with sodium hydroxide and get start to dissolve along with the formation of traces of the sodium salt of the cellulose. As can be seen, the overall shape of all diffraction patterns is quite similar except untreated raw fibre. On removing the noncrystalline constituents (lignin & hemicellulose) from the fibres by chemical treatment, the degree of crystallinity and crystallinity index will change with a positive shift.

Degree of crystallinity of the fibre goes on increasing in both the processing stages. This may be due to the removal of lignin which acts as a cementing material and on delignification, an ordered arrangement of the crystalline cellulose in the structure takes place. The XRD pattern of bleached fiber, where the crystallinity is increased, gives a relatively intense peak at 2θ , 22.5° . During the bleaching step, the lignin will dissolve out as lignin chloride and the cellulose component will leave without intact. Increase in the percentage crystallinity in the fibers is due to the fact that during acid treatment the amorphous regions are readily attacked by dilute acid while the crystalline regions are more resistant to attack.

4.6 Zeta potential measurements

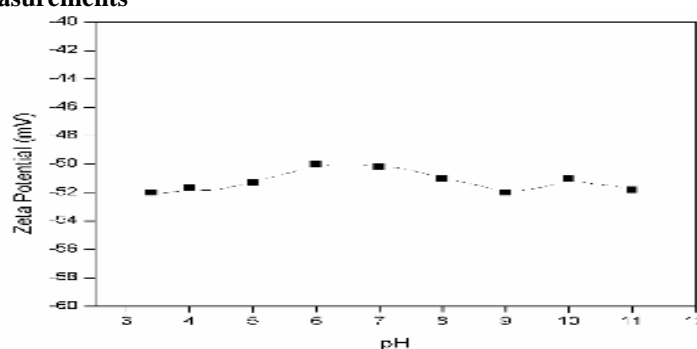


Figure 5: Zeta potential measurements of cellulose nanowhiskers

The zeta potential is an important parameter for examining dispersion stability. The pH dependence of the zeta potential was determined in a 1×10^{-3} M KCl electrolyte solution and, to keep the ionic strength constant, the pH value in the range 3-11 was altered by the addition of 0.1 M HCl or KOH solution. The characterization of solid surfaces by electrokinetic phenomena was reported by Jacobasch [37], Stana-Kleinschek and Ribitsch [38], discussed the electrokinetic properties of processed cellulose fibers. Zeta potential measurements were carried out on aqueous dispersions of relevant microfibrillar cellulose samples, prepared under the specified hydrolysis conditions. Relevant data are given in figure 5. It is important to note that, insufficient hydrolysis of cellulose may result in larger particles (less surface area per unit mass) with a lower mean surface charge, favouring particle-particle interaction (Hebeish & Guthrie, 1981). Zeta potential is due to the formation of the electric double layer between a solid substrate and a liquid electrolyte. Here it is a measure of the mobility distribution of the dispersion of charged nanocellulose particles as they are subjected to an electric field. Thus the successful introduction of sulfate groups can be easily followed by determinations of the zeta potential of these suspensions. As expected, the CNC whiskers exhibit a highly negative zeta potential over a wide pH range.

4.7 Determination of Red Blood Cells' Mobility

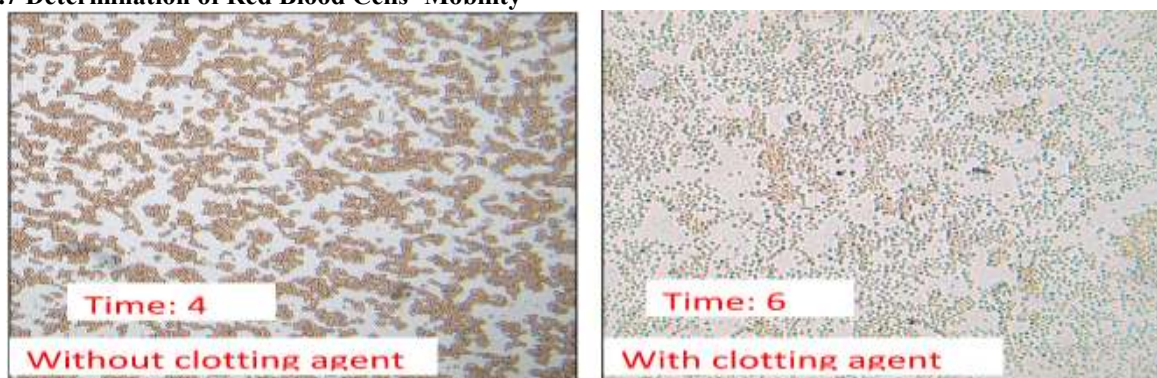


Figure 6: Optical microscopy images of red blood cells with and without cellulose nanowhiskers as clotting agent.

Figure 6 shows the results of the mobility determination of erythrocytes in whole blood with and without cellulose nanowhiskers. The mobility time range of the coated surfaces is significantly higher when compared to the non-coated surface. The picture with cellulose nanocrystals shows only round 'normal' erythrocytes with a regular cell membrane and they are not too close together [39-40]. In the case of the non-coated surface, the erythrocytes transform into echinocytes, the cell membrane forms tentacles and the erythrocytes are settled very close together. After some time, the mobility of erythrocytes on the non-coated surface stopped, but on the surfaces CNC coated surfaces, erythrocytes were still able to move around and their mobility only stopped after 6 min. This results proved the efficiency of prepared cellulose nanowhiskers as an anticoagulant.

V. CONCLUSIONS

- Cellulose nanocrystals from renewable date palm leaves were produced and characterized.
- Specific functionalization of cellulose nanowhisiker by sulphate groups was performed.
- Anticoagulant effect of functionalized cellulose nanocrystals was demonstrated by clinical test.
- This new material is potentially applicable in medicine as anticoagulant similarly as common heparin

REFERENCES

- [1]. J. F. Revol, H. Bradford, J. Giasson, R. H. Marchessault and D. G. Gray, *Int. J. Biol. Macromol.*, 1992, 14, 170.
- [2]. S. J. Eichhorn, A. Dufresne, *Nature Nanotech.* 2007, 2, 765.
- [3]. Habibi, Y., Lucia, L. A., & Rojas, O. J. (2010). Cellulose nanocrystals: Chemistry, selfassembly, and applications. *Chemical Reviews*, 110(6), 3479–3500.
- [4]. Lima, M. M. D., & Borsali, R. (2004). Rodlike cellulose microcrystals: Structure, properties, and applications. *Macromolecular Rapid Communications*, 25, 771–787.
- [5]. Samir, M. A. S. A., Alloin, F., & Dufresne, A. (2005). Review of recent research into cellulosic whiskers, their properties and their application in nanocomposite field. *Biomacromolecules*, 6(2), 612–626.
- [6]. S. Dong, A. A. Hirani, K. R. Colacino, Y. W. Lee and M. Roman, *Nano LIFE*, 2012, 2, 1241006
- [7]. Gardner DJ, Oporto GS, Mills R, Samir MASA (2008) Adhesion and Surface Issues in Cellulose and Nanocellulose. *J AdhesSciTechnol* 22:545–567
- [8]. Hubbe MA, Rojas OJ, Lucia LA, Sain M (2008) Cellulosic nanocomposites, review. *BioResources* 3(3):929–980
- [9]. Samir MASA, Alloin F, Dufresne A (2005) Review of recent research into cellulosic whiskers, their properties and their application in nanocomposite field. *Biomacromolecules* 6(2):612–626
- [10]. H. M. A. Ehmann, T.S. Mohan, M. Koshanskaya, S. Scheicher, D. Breitwieser, V. Ribitsch, S. Kleinschek, S. Spirk, *ChemComm*, DOI: 10.1039/c4cc05254d
- [11]. Yasushi, T. Sulfation of silk fibroin by chlorosulfonic acid and the anticoagulant activity. *Biomaterials* 2004, 25, 377–384
- [12]. Alban, S.; Schauerte, A.; Franz, G. Anticoagulant sulfated polysaccharides: part I. Synthesis and structure-activity relationship of new pullulan sulfates. *Carbohydr. Polym.* **2002**, 47, 267–276.
- [13]. Warkentin, T.E.; Chong, B.H.; Greinacher, A. Heparin-induced thrombocytopenia: towards consensus. *Thromb. Haemost.* **1998**, 79, 1–7.
- [14]. Ye, L.; Xu, L.; Li, J. Preparation and anticoagulant activity of a fucosylated polysaccharide sulfate from a sea cucumber *Acaudinamolpadioidea*. *Carbohydr. Polym.* **2012**, 87, 2052–2057.
- [15]. Sinay, P.; Jacquinet, J.C.; Petitou, M.; Duchaussoy, P.; Lederman, I.; Choay, J.; Torri, G. Total synthesis of a heparin pentasaccharide fragment having high affinity for antithrombin III. *Carbohydr. Res.* **1984**, 130, 221–241.
- [16]. El Hadrami, I. and A. El Hadrami. 2009 Breeding date palm. pp. 191-216. In: Jain S.M. and P.M. Priyadarshan (Eds.) *Breeding Plantation Tree Crops*, Springer, New York.
- [17]. Jain, S. M., J. M. Al-Khayri and D.V. Johnson. (Eds.) 2011. *Date Palm Biotechnology*.
- [18]. Springer, Netherlands
- [19]. S. Lahooti, H. K. Yueh and A. W. Neumann, *Colloids Surfaces B: Biointerfaces* 3, 333 (1995)
- [20]. Erdtman, H. (2003). Lignins: Occurrence, formation, structure and reactions *Journal of Polymer Science Part B: Polymer Letters*, 10, 228–230
- [21]. Klemm, D., Philipp, B., Heinze, T., Heinze, U., & Wagenknecht, W. (2004). General Considerations on Structure and Reactivity of Cellulose: Section 2.4–2.4.3 *Comprehensive Cellulose Chemistry, Volume 1*, Wiley-VCH Verlag GmbH, p 130-165
- [22]. Fernfindez, J.B., Felizon, B., Heredia, A., Guillen, R., Jimenez, A., 1999. Characterization of the lignin obtained by alkaline delignification and of the cellulose residue from steam-exploded olive stones. *Bioresour. Technol.* 68, 121–132

- [23]. Jiebing, L., Gunnar, H., Goran, G., 2007. Lignin depolymerization/repolymerization and its critical role for delignification of aspen wood by steam explosion. *Biore-sour. Technol.* 98, 3061–3068.
- [24]. Xiao, B., Sun, X.F., Sun, R.C., 2001. Chemical, structural and thermal characterization of alkali-soluble lignins and hemicelluloses and cellulose from maize stems and rice straw. *Polym. Degrad. Stab.* 74, 307–319.
- [25]. Dufresne, A., Caville, J., Vignon, M., 1997. Mechanical behavior of sheets prepared from sugar beet cellulose microfibrils. *J. Appl. Polym. Sci.* 64, 1185–1194
- [26]. Rodriguez, N.L.G., Thielemans, W., Dufresne, A., 2006. Sisal cellulose whiskers reinforced polyvinyl acetate nanocomposites. *Cell* 13, 261–270
- [27]. Klemm, D., Schumann, D., Kramer, F., Hebler, N., Hornung, M., & Marsch, S. 468 (2006). Nanocelluloses as innovative polymers in research and application. *Advanced 469 Polymer Science*, 205, 49–96
- [28]. Erdtman, H. (2003). Lignins: Occurrence, formation, structure and reactions. *Journal of Polymer Science. Part B: Polymer Letters*, 10, 228 – 230
- [29]. Klemm, D., Philipp, B., Heinze, T., Heinze, U., & Wagenknecht, W. (2004). 465 *Comprehensive Cellulose Chemistry, Volume 1*, Wiley-VCH Verlag GmbH, Section 466 2.4–2.4.3
- [30]. Oh, S. Y., Yoo, D. I., Shin, Y., & Seo, G. (2005). FTIR analysis of cellulose treated with sodium hydroxide and carbon dioxide. *Carbohydrate Research*, 340, 417–428.
- [31]. Hatem, M.; Mohamed, B.M.; Frédéric, C.; Mohamed, S.R.; Raoui, M.M. Anticoagulant activity of a sulfated polysaccharide from the green alga *Arthrospiraplatensis*. *Biochem. Biophys. Acta* 2009, 1790, 1377–1381.
- [32]. Moran, J.I., Alvarez, V.A., Viviana, P.C., Vazquez, A., 2008. Extraction of cellulose and preparation of nanocellulose from sisal fibers. *Cellulose* 15, 149–159.
- [33]. Moran, J.I., Alvarez, V.A., Viviana, P.C., Vazquez, A., 2008. Extraction of cellulose and preparation of nanocellulose from sisal fibers. *Cellulose* 15, 149–159.
- [34]. Moran, J.I., Alvarez, V.A., Viviana, P.C., Vazquez, A., 2008. Extraction of cellulose and preparation of nanocellulose from sisal fibers. *Cellulose* 15, 149–159.
- [35]. Battista, O. A., & Smith, P. A. (1962). *Industrial and Engineering Chemistry*, 54, 20–29.
- [36]. Lai-Kee-Him, H., Chanzy, H., Müller, M., Putaux, J.-L., Imai, T., & Bulone, V. (2002). In vitro versus in vivo cellulose microfibrils from plant primary wall synthases: Structural differences. *The Journal of Biological Chemistry*, 277(40), 36931–36939
- [37]. Dong, X. M., Revol, J.-F., & Gray, D. G. (1998). Effect of microcrystalline preparation conditions on the formation of colloid crystals of cellulose. *Cellulose*, 5, 19–32.
- [38]. Jacobasch, H. J.; Simon, F.; Werner, C.; Bellmann, C. *Tech. Mess.* 1996, 63, 439–447.
- [39]. Stana-Kleinschek, K.; Ribitsch, V. *Colloids Surf., A* 1998, 140, 127–138.
- [40]. Hebeish, A., & Guthrie, J. T. (1981). *The chemistry and technology of cellulosic copolymers*. New York: Springer-Verlag.
- [41]. Aleš Doliška, Simona Strnad, Jan Stana, Elisabeth Martinelli, Volker Ribitsch & Karin Stana-Kleinschek (2012) In Vitro Haemocompatibility Evaluation of PET Surfaces Using the Quartz Crystal Microbalance Technique, *Journal of Biomaterials Science, Polymer Edition*, 23:5, 697-714, DOI: 10.1163/092050611X559232